Research Square

Preprints are preliminary reports that have not undergone peer review.
They should not be considered conclusive, used to inform clinical practice,
or referenced by the media as validated information.

# Value of Amide Proton Transfer Imaging Combined with Diffusion-Weighted Imaging and Clinical Indicators for Predicting Treatment Response in Cervical Squamous Cell Carcinoma

**Shanyu Fang**
Jiangsu Cancer Hospital, Nanjing Medical University
**Feng Dai**
Intervention Department,Nanjing Second Hospital
**Hanzi Xu**
Jiangsu Cancer Hospital, Nanjing Medical University
**Qianlai Jiang**
Department of Radiology, Liyang Branch of Jiangsu Province Hospital of Chinese Medicine
**Yunnong Wang**
Department of Radiology, BenQ Medical Center, the Affiliated BenQ Hospital of Nanjing Medical University
**Xiuming Zhang**
zhangxiuming360@163.com
Jiangsu Cancer Hospital, Nanjing Medical University
**Na Yin**
Jiangsu Cancer Hospital, Nanjing Medical University

**Research Article**

**Keywords:** cervical cancer, MRI, APT, DWI, treatment response prediction

**Posted Date:** November 26th, 2026

**DOI:** https://doi.org/10.21203/rs.3.rs-11512700/v1

**License:** This work is licensed under a Creative Commons Attribution 4.0 International License.
Read Full License

**Additional Declarations:** No competing interests reported.

# Abstract

**Objective:** To investigate the value of a predictive model integrating amide proton transfer (APT)-weighted imaging, diffusion-weighted imaging (DWI), and clinical indicators for predicting the response to concurrent chemoradiotherapy (CCRT) in patients with cervical squamous cell carcinoma (SCC).

**Methods:** A total of 66 patients with pathologically confirmed SCC were retrospectively enrolled. All patients underwent APT and DWI magnetic resonance imaging and had clinical data collected before CCRT. Based on the Response Evaluation Criteria in Solid Tumors (RECIST), version 1.1, patients were classified into a response group (n = 40) and a non-response group (n = 26). Logistic regression analysis was used to develop predictive models, and receiver operating characteristic (ROC) curve analysis was performed to evaluate their predictive performance. Net reclassification improvement (NRI) and integrated discrimination improvement (IDI) were used to assess the incremental predictive value of the models. Internal validation was performed using 1,000 bootstrap resamplings.

**Results:** The ADC values of the 66 patients with cervical SCC increased significantly after concurrent chemoradiotherapy (CCRT) compared with those before treatment [$(0.85 \pm 0.11) \times 10^{-3}$ $mm^2/s$ vs. $(0.88 \pm 0.21) \times 10^{-3}$ $mm^2/s$, $P < 0.05$], whereas APT values decreased significantly (3.72% ± 0.31% vs. 3.62% ± 0.64%, $P < 0.03$). After CCRT, the response group had significantly higher ADC values than the non-response group [$(0.92 \pm 0.20) \times 10^{-3}$ $mm^2/s$ vs. $(0.81 \pm 0.21) \times 10^{-3}$ $mm^2/s$, $P < 0.01$], whereas APT values were significantly lower (3.47% ± 0.62% vs. 3.84% ± 0.61%, $P < 0.01$). The areas under the ROC curve (AUCs) for Model 1 (clinical variables), Model 2 (clinical variables + ADC), and Model 3 (clinical variables + ADC + APT) were 0.701, 0.785, and 0.845, respectively ($P < 0.05$). Compared with Model 2, Model 3 demonstrated an NRI of 0.558 ($P < 0.05$) and an IDI of 0.118 ($P < 0.01$). After 1,000 bootstrap resampling iterations for internal validation, the bias-corrected AUC was 0.793.

**Conclusion:** In patients with cervical SCC, a favorable response to CCRT was associated with increased ADC values and decreased APT values. The predictive model integrating APT, DWI-derived ADC, and clinical variables demonstrated good performance in predicting treatment response.


# 1. Introduction

Cervical cancer is one of the most common malignancies in women and remains a major threat to women's health worldwide [1]. Squamous cell carcinoma (SCC) is the most common histological type of cervical cancer, accounting for approximately 75% of cases [2]. Concurrent chemoradiotherapy (CCRT) is recommended by the National Comprehensive Cancer Network guidelines as the standard treatment for locally advanced cervical cancer. However, owing to tumor heterogeneity, some patients respond poorly to CCRT. Therefore, predicting treatment response is essential for treatment planning and prognostic assessment [3],[4]. MRI offers several advantages in localizing cervical lesions, measuring tumor size, and assessing parametrial involvement and lymph node metastasis. However, anatomical tumor volume does not always correspond to metabolic tumor volume, and anatomical measurements alone may

therefore be insufficient to accurately predict treatment response [5]–[7]. Diffusion-weighted imaging (DWI) has been used to address this limitation, although some studies have reported that it has its own limitations [8]. Amide proton transfer (APT) imaging is an emerging molecular MRI technique that provides information related to mobile proteins and peptides in tissues. In this study, APT imaging was combined with DWI and clinical indicators to evaluate treatment response before and after CCRT in patients with cervical SCC. Although previous studies have begun to explore the use of APT imaging for response assessment in cervical cancer [9],[10], whether integrating APT, DWI, and clinical indicators improves the prediction of CCRT response in cervical SCC remains unclear. Accordingly, this study compared the predictive performance of three models: one based on clinical indicators alone, one combining clinical indicators with DWI-derived ADC values, and one integrating clinical indicators, ADC values, and APT imaging.

## 2. Materials and Methods

# 2.1 Study population

This retrospective study included patients with FIGO stage IIB–IVA cervical SCC who received CCRT at the Affiliated Cancer Hospital of Nanjing Medical University between November 2024 and June 2025. Clinical and imaging data from 66 patients with histopathologically confirmed SCC were analyzed.

The inclusion criteria were as follows: (1) histopathological confirmation of SCC by cervical biopsy; (2) no history of surgery, radiotherapy, or chemotherapy before the initial MRI examination; (3) availability of complete routine MRI, APT, and DWI sequences, with MRI performed before CCRT or within one week after one course of CCRT; and (4) receipt of standardized CCRT at the study hospital and availability of complete clinical records. The exclusion criteria were as follows: (1) histological types other than SCC; (2) loss to follow-up or incomplete clinical records; and (3) MRI images of insufficient quality for assessment. The study was approved by the Ethics Committee of the Affiliated Cancer Hospital of Nanjing Medical University (approval No. 2021-005).All person information was anonymized during the study.

# 2.2 Clinical data and MRI acquisition

# 2.2.1 Clinical data

Baseline clinical data were obtained from the hospital medical record system, including age, FIGO stage, maximum pretreatment tumor diameter, pretreatment hemoglobin (Hb) level, and pretreatment serum squamous cell carcinoma antigen (SCC-Ag) level.

# 2.2.2 MRI equipment and acquisition

All patients underwent pretreatment MRI examinations using a 3.0-T Philips Ingenia scanner (Philips, the Netherlands) equipped with a 16-channel phased-array body coil. Patients fasted and abstained from

drinking for 4–6 hours before the examination to reduce bowel peristalsis and drank approximately 500 mL of water 1 hour before scanning to achieve moderate bladder filling. The scan range extended from the superior border of the uterus to below the pubic symphysis. The MRI sequences and acquisition parameters are presented in Table 1.

Table 1
MRI sequences and acquisition parameters.

| Sequence | TR/ms | TE/ms | FOV ($mm^2$) | Voxel ($mm^2$) | Matrix | Slice thickness (mm) | Gap (mm) | Scan time |
|---|---|---|---|---|---|---|---|---|
| T1WI | 505 | 10 | 260×350 | 1×1 | 300×280 | 5 | 0 | 60 s |
| T2WI | 2600 | 100 | 260×350 | 1×1 | 380×240 | 5 | 0 | 2 min |
| DWI | 1700 | 80 | 350×350 | 3×3 | 130×120 | 5 | 0 | 90 s |
| APT | 10000 | 10 | 200×200 | 2×2 | 100×100 | 7 | 7 | 5 min |

## 2.3 Image analysis and quantitative measurements

Two experienced gynecologic radiologists independently assessed image quality. Images that met the quality criteria were transferred to a Philips workstation for post-processing and generation of parametric maps. Axial and sagittal T2-weighted images and axial DWI images (b = 1,000 s/$mm^2$) were used as anatomical references. A region of interest (ROI) was manually delineated on the slice showing the largest tumor cross-section, and the ADC and APT values were measured three times, with the results averaged for analysis. Necrotic and hemorrhagic areas were excluded, and ROI locations were kept as consistent as possible between the ADC and APT maps. For post-treatment images, measurements were performed at the corresponding pretreatment tumor level whenever possible. If the lesion had shrunk to a size smaller than the original ROI or had completely disappeared, measurements were obtained from the pretreatment tumor location. The original manuscript contains an unresolved editorial comment regarding the stated ROI area (approximately 55 $mm^2$); the authors should verify this measurement rule and clarify how ROIs were handled when lesions were smaller.

## 2.4 Treatment response assessment

Two gynecologic radiologists independently assessed tumor response by comparing pretreatment and post-treatment T2-weighted images under blinded conditions. Treatment response was classified according to the Response Evaluation Criteria in Solid Tumors (RECIST) version 1.1, as complete response (CR; disappearance of the target lesion), partial response (PR; a decrease of at least 30% in the longest diameter of the target lesion), progressive disease (PD; an increase of at least 20% in the longest diameter of the target lesion), or stable disease (SD; neither sufficient tumor shrinkage to qualify as PR nor sufficient tumor growth to qualify as PD). Patients with CR or PR were assigned to the response group, whereas those with SD or PD were assigned to the non-response group.

## 2.5 Statistical analysis

Statistical analyses were performed using SPSS version 27.0 and R software. Normally distributed continuous variables were expressed as mean ± standard deviation. Between-group differences were assessed using the independent-samples *t*-test, whereas within-patient changes between time points were evaluated using the paired *t*-test. Categorical variables were presented as counts and percentages and compared using Pearson's chi-square test. The Shapiro–Wilk test was used to assess normality. Normally distributed continuous variables were analyzed using the independent-samples *t*-test, while non-normally distributed variables were analyzed using the Mann–Whitney U test.

Logistic regression was used to develop predictive models incorporating APT, DWI-derived ADC, and clinical indicators. Receiver operating characteristic (ROC) curve analysis and ROC curve values were used to evaluate the predictive performance of the models for CCRT response. Net reclassification improvement (NRI) and integrated discrimination improvement (IDI) were calculated to assess the incremental predictive value of the models. Internal validation was performed using 1,000 bootstrap resamples, and the bias-corrected area under the ROC curve (AUC) was calculated. A two-sided P value of < 0.05 was considered statistically significant.

# 3. Results

### 3.1 Comparison of APT and ADC values before and after CCRT

ADC values increased significantly after CCRT, whereas APT values decreased significantly (Table 2). Note: There are minor inconsistencies in the reported ADC summary statistics across sections of the manuscript, including post-treatment mean values of 0.87 versus 0.88 × $10^{-3}$ $mm^2/s$ and pretreatment standard deviations of 0.10 versus 0.11. These values should be verified against the original statistical output and reconciled before submission.

Table 2. Comparison of APT and ADC values before and after CCRT in patients with cervical SCC.

| Parameter | Before CCRT | After CCRT | *t* value | *p* value |
|---|---|---|---|---|
| APT% | 3.72 ± 0.31 | 3.62 ± 0.64 | 2.38 | 0.02 |
| ADC/(×$10^{-3}$ $mm^2/s$) | 0.85 ± 0.11 | 0.88 ± 0.21 | 2.22 | 0.03 |

### 3.2 Comparison of APT and ADC values between response groups

Both before and after CCRT, the response group exhibited higher ADC values and lower APT values than the non-response group, with statistically significant differences between the groups (Table 3).

Table 3. Comparison of APT and ADC values before and after CCRT between the response and non-response groups.

| Group | APT(%) | | ADC×$10^{-3}$ $mm^2/s$ | |
|---|---|---|---|---|
| | Before CCRT | After CCRT | Before CCRT | After CCRT |
| Response (n = 40) | 3.59 ± 0.27 | 3.47 ± 0.62 | 0.88 ± 0.09 | 0.92 ± 0.20 |
| Non-response (n = 26) | 3.92 ± 0.26 | 3.84 ± 0.61 | 0.79± 0.10 | 0.81± 0.21 |
| t | 5.10 | 2.43 | 3.83 | 2.27 |
| p | <0.001 | 0.018 | <0.001 | 0.027 |

## 3.3 Comparison of baseline characteristics between response groups

Comparison of baseline clinical and pretreatment imaging characteristics revealed significant differences in pretreatment SCC-Ag, ADC, and APT values between the response and non-response groups (all P < 0.05). In contrast, no significant differences were observed in FIGO stage, maximum tumor diameter, or Hb levels between the groups (all P > 0.05) (Table 4).

Table 4. Baseline characteristics of the response and non-response groups.

| Characteristic | Response (n=40) | Non-response (n=26) | Statistic | P value |
|---|---|---|---|---|
| FIGO 2018 stage | | | $\chi^2$=3.320 | 0.817 |
| IIA | 1（2.5%） | 1（3.8%） | | |
| IIB | 7（17.5%） | 1（3.8%） | | |
| IIIA | 1（2.5%） | 1（3.8%） | | |
| IIIB | 13（32.5%） | 11（42.3%） | | |
| IIIC1 | 11（27.5%） | 8（30.8%） | | |
| IIIC2 | 6（15.0%） | 3（11.5%） | | |
| IVA | 1（2.5%） | 1（3.8%） | | |
| Maximum tumor diameter (cm) | 3.83 ± 0.98 | 4.23 ± 1.23 | t=-1.442 | 0.154 |
| Pretreatment Hb（g/L） | 111.95（105.05，126.78） | 111.00（100.02，114.70） | U=667.000 | 0.055 |
| Pretreatment SCC-Ag （ng/mL） | 5.68（4.01，12.08） | 10.21（6.73，22.34） | U=337.000 | 0.017 |
| Pretreatment ADC （$\times10^{-3}$ $mm^2/s$） | 0.88± 0.09 | 0.79± 0.10 | t=3.83 | <0.01 |
| Pretreatment APT(%) | 3.59 ± 0.27 | 3.33 ± 0.26 | t=6.57 | <0.01 |

FIGO: International Federation of Gynecology and Obstetrics; Hb: hemoglobin; SCC-Ag: squamous cell carcinoma antigen.

# 3.4 Development and performance of the predictive models

## 3.4.1 Model development

The clinical indicators included FIGO stage, maximum tumor diameter, Hb level, and SCC-Ag level, while the imaging indicators comprised mean APT and ADC values. Model 1 included the clinical indicators alone; Model 2 incorporated the clinical indicators and mean ADC value; and Model 3 incorporated the clinical indicators, mean ADC value, and mean APT value.

### 3.4.2 Predictive performance

ROC analysis yielded AUCs of 0.701 (95% confidence interval [CI], 0.569–0.833), 0.785 (95% CI, 0.664–0.905), and 0.845 (95% CI, 0.745–0.945) for Models 1, 2, and 3, respectively. Model 3, which incorporated APT, demonstrated the best discriminative performance among the three models (Figure 2).

### 3.4.3 Incremental predictive value

NRI and IDI were used to evaluate the incremental predictive value of the models. Compared with Model 1, Model 2, which incorporated ADC alongside the clinical indicators, improved discrimination between predicted probabilities (IDI = 0.121, P = 0.002). Compared with Model 2, Model 3, which additionally incorporated APT, yielded a continuous NRI of 0.558 (95% CI, 0.069–1.020; P = 0.028) and an IDI of 0.118 (95% CI, 0.041–0.191; P = 0.002), indicating improved risk classification and an 11.8% increase in discrimination (Table 5).

Table 5. Comparison of continuous NRI and IDI.

| **Model comparison** | **Continuous NRI** | NRI 95%CI | NRI P **value** | IDI | IDI 95%CI | IDI P **value** |
|---|---|---|---|---|---|---|
| Model 1 vs Model 2 | 0.458 | −0.023–0.889 | 0.070 | 0.121 | 0.045–0.189 | 0.002 |
| Model 2 vs Model 3 | 0.558 | 0.069–1.020 | 0.028 | 0.118 | 0.041–0.191 | 0.002 |

NRI: net reclassification improvement; IDI: integrated discrimination improvement

## 3.5 Calibration, internal validation, and clinical utility

Calibration curve analysis indicated good agreement between the probabilities predicted by Model 3 and the observed probabilities of non-response. After 1,000 bootstrap resamples, the bias-corrected AUC was 0.793, lower than the apparent AUC of 0.845. This reduction suggests a degree of overfitting, although the bias-corrected AUC indicates that the model retained useful discriminative ability.

Decision curve analysis (DCA) was performed to evaluate the potential clinical benefit of the models (Figures 3 and 4). Across most threshold probabilities, Model 3 demonstrated a greater net benefit than Models 1 and 2, suggesting that integrating APT with DWI-derived ADC values and clinical indicators may improve the clinical utility of predicting treatment response.

## 4. Discussion

Advances in MRI have expanded its role beyond conventional anatomical assessment to include the characterization of tumor metabolism and the microenvironment [7]. Functional MRI provides microscopic and metabolic information that cannot be obtained from conventional MRI alone [11]–[13].

Cervical SCC is heterogeneous, and sensitivity to CCRT varies considerably among patients [4]. Accurate assessment of treatment response and identification of patients likely to benefit from therapy are therefore essential for optimizing treatment strategies and supporting individualized care. Conventional MRI mainly evaluates treatment effects through changes in tumor size, morphology, and signal intensity. However, anatomical changes may lag behind cellular and molecular alterations, and tumor volume alone may not adequately reflect tumor biology. Accordingly, this study investigated APT imaging and developed predictive models integrating APT, DWI, and clinical indicators to predict CCRT response in patients with cervical SCC.

In this cohort of 66 patients with pathologically confirmed cervical SCC, treatment response was classified according to RECIST version 1.1. Following CCRT, ADC values increased, whereas APT values decreased. Compared with the non-response group, the response group exhibited higher post-treatment ADC values and lower post-treatment APT values. Pretreatment SCC-Ag levels were also lower in the response group, and significant between-group differences were observed in pretreatment ADC and APT values. The AUCs of the clinical model, the clinical-plus-ADC model, and the model integrating clinical indicators, ADC, and APT were 0.701, 0.785, and 0.845, respectively. These findings suggest that incorporating functional MRI parameters progressively improved predictive performance, with APT providing additional predictive value beyond clinical indicators and ADC.

DWI is a widely used functional MRI technique that characterizes tissue microstructure by measuring the random motion of water molecules. The ADC quantifies the degree of water diffusion [14]. Tumors often exhibit high cellularity, enlarged nuclei, and reduced extracellular space, which restrict water diffusion and result in lower ADC values than those of normal tissues. Following chemoradiotherapy, tumor cell apoptosis and necrosis may reduce cellularity and expand the extracellular space, facilitating water diffusion and increasing ADC values. Therefore, ADC can reflect microstructural changes associated with the response to CCRT [8]. In the present study, pretreatment ADC values were significantly higher in the response group than in the non-response group ($0.88 \pm 0.09$ vs. $0.79 \pm 0.10 \times 10^{-3}$ $mm^2/s$; $P < 0.001$), suggesting an association between baseline ADC and subsequent treatment response. Previous DWI studies in cervical cancer have also reported associations between ADC values, tumor cellularity, and treatment response [15]. Zhang et al. found that changes in ADC during treatment were associated with the final treatment response [16]. In our study, incorporating ADC into the clinical model increased the AUC from 0.701 to 0.785, with an IDI of 0.121 ($P = 0.002$). These findings support the value of DWI-derived microstructural information as a complement to conventional clinical indicators for predicting CCRT response.

APT imaging is a functional MRI technique based on chemical exchange saturation transfer. It uses exchangeable amide protons to provide indirect information about mobile proteins and peptides in tissues, potentially reflecting cellular proliferation, metabolism, and the tissue microenvironment [17]. APT imaging has increasingly been investigated in cervical cancer for histological grading, pathological characterization, and treatment response assessment [18]–[20]. Previous studies have suggested that APT

imaging may be valuable for evaluating histological subtype, SCC differentiation, and lymph node involvement [18],[21],[22]. In the present study, APT values decreased after CCRT and were significantly lower in the response group than in the non-response group after treatment. These findings may reflect treatment-related tumor cell death, reduced cellularity and heterogeneity, and changes in protein and peptide content. Treatment-induced changes in vascularity, oxygenation, and tissue pH may also influence APT signals, although these potential mechanisms require further investigation[18],[19].

The association between pretreatment APT values and treatment sensitivity should be interpreted cautiously[17]. APT signals are sensitive to mobile proteins and peptides in tissues, and active tumor cell proliferation and protein synthesis may increase the concentration of exchangeable amide protons, resulting in higher APT values. Conversely, tumors with different levels of biological activity or treatment sensitivity may exhibit distinct protein metabolism and proliferation profiles [17],[20]. In the present study, adding APT to Model 2 increased the AUC from 0.785 to 0.845. The continuous NRI was 0.558 (95% CI, 0.069–1.020; P = 0.028), and the IDI was 0.118 (95% CI, 0.041–0.191; P = 0.002), indicating improvements in risk classification and discriminative performance. These findings suggest that APT and ADC characterize different aspects of tumor biology and may provide complementary information for predicting CCRT response.

A single functional MRI parameter captures only part of a tumor's biological characteristics[8]. Response to CCRT is influenced by multiple factors, including tumor cellularity, proliferative capacity, metabolism, the tumor microenvironment, and patient-related characteristics [3]. Integrating multidimensional information may therefore improve predictive performance. In this study, we developed three models: Model 1 incorporated FIGO stage, maximum tumor diameter, Hb level, and SCC-Ag level; Model 2 additionally included ADC; and Model 3 further incorporated APT. Model 3 achieved the highest AUC (0.845; 95% CI, 0.745–0.945), supporting the potential value of combining APT, DWI, and clinical indicators for predicting treatment response. Research is increasingly shifting from single-parameter functional MRI toward multiparametric approaches. In 2025, Yang et al. reported that combining APT, ADC, and dynamic contrast-enhanced MRI (DCE-MRI) parameters in patients with locally advanced cervical cancer achieved an AUC of 0.893, outperforming individual parameters [23]. Although our study included a relatively small sample, the AUC of 0.845 further supports the potential complementary value of multiparametric MRI and clinical data for predicting CCRT response.

Discrimination alone does not establish the accuracy of a prediction model in estimating individual risk; calibration and clinical net benefit should also be evaluated [24]. In this study, the calibration curve showed reasonable agreement between the predicted and observed probabilities of non-response. After 1,000 bootstrap resamples, the bias-corrected AUC decreased from 0.845 to 0.793. Although this reduction suggests some degree of overfitting, the bias-corrected AUC indicates that the model retained useful discriminative ability. Nevertheless, external validation in an independent cohort is required to further assess the model's generalizability.

DCA evaluates the potential clinical utility of a prediction model by assessing its net benefit across a range of threshold probabilities, rather than focusing solely on statistical performance. In this study, Model 3 demonstrated greater net benefit than Models 1 and 2 across most threshold probabilities, suggesting that the combined model may provide clinically useful information. If validated in independent cohorts, Model 3 could be used before treatment to help identify patients at risk of a poor response to CCRT and inform individualized treatment planning.

This study has several limitations. First, the relatively small sample size may have increased the risk of overfitting. Although internal validation was performed using bootstrap resampling, independent external validation has not yet been conducted, and the generalizability of the model remains uncertain. Second, the manual delineation of ROIs may have introduced measurement variability. Future studies could employ whole-tumor volumetric analysis, histogram analysis, or radiomics to extract more comprehensive quantitative features. Third, treatment response was classified according to RECIST version 1.1, with patients achieving CR or PR assigned to the response group and those with SD or PD assigned to the non-response group. Although this approach provides a morphological assessment of treatment response, tumor shrinkage does not necessarily translate into durable local control or improved survival. Future studies should incorporate progression-free survival, local control, and overall survival as clinical endpoints to further establish the prognostic value of APT, ADC, and the combined predictive model.

# 5. Conclusion

In patients with cervical SCC, response to CCRT was associated with increased ADC values and decreased APT values. MRI provides valuable information for assessing treatment response. A predictive model integrating APT, DWI-derived ADC, and clinical indicators combines complementary information on tumor microstructure, metabolic characteristics, and clinical status. The model demonstrated promising discriminative performance, good calibration, internal stability, and potential clinical utility, suggesting that it may serve as an imaging-based tool for pretreatment prediction of CCRT response. However, further external validation is required before clinical implementation.

# Declarations

### Data availability statement

The original data and findings supporting this study are provided in the article and its Supplementary Materials. Further information may be obtained from the corresponding author upon request.

### Ethics statement

The studies involving humans were approved by the Ethics Committee of the Affiliated Cancer Hospital of Nanjing Medical University (approval No. 2021-005). The studies were conducted in accordance with

the local legislation and institutional requirements.Written informed consent for participation in this study was provided by the participants' legal guardians/next of kin.

**Author contribution**

SF: Conceptualization, Data collection, Formal Analysis, Funding acquisition, Investigation, Methodology, Project administration, Resources, Software, Supervision, Validation,Visualization, Writing-original draft, Writing-review&editing. FD: Conceptualization, Data collection, Formal Analysis, Funding acquisition, Investigation, Methodology, Project administration, Resources, Software, Supervision, Validation, Visualization, Writing-original draft,Writing-review&editing. HX: Conceptualization, Data collection,Writing-review&editing. QJ: Methodology, Project administration, Resources. YW: Conceptualization, Data collection, Formal Analysis. XZ: Conceptualization, Data collection, Formal Analysis, Funding acquisition, Investigation, Methodology, Project administration, Resources, Software, Supervision, Validation,Visualization,Writing-original draft, Writing-review&editing. NY: Conceptualization, Data collection, Formal Analysis, Funding acquisition, Investigation, Methodology, Project administration, Resources, Software, Supervision, Validation,Visualization,Writing-original draft, Writing-review&editing.

**Funding**

The author(s) declare that no financial support was received for the research and/or publication of this article.

**Conflict of interest**

The authors declare that the research was conducted in the absence of any commercial or financial relationships that could be construed as a potential conflict of interest.

**Publishers' note**

All claims expressed in this article are solely those of the authors and do not necessarily represent those of their affiliated organizations, or those of the publisher, the editors and the reviewers.Any product that may be evaluated in this article,or claim that made by its manufacturer,is not guaranteed or endorsed by the publisher.

**Consent for publication**

Not applicable. The manuscript does not contain any individual person's data in any form (including individual details, images or videos) that could compromise patient anonymity.

# References

1. Voelker RA. Cervical Cancer Screening[J]. JAMA, 2023, 330(20): 2030.

2. Tsikouras P, Zervoudis S, Manav B, et al. Cervical cancer: screening, diagnosis and staging[J]. J B U : official J Balkan Union Oncol. 2016;21(2):320–5.
3. Abu-Rustum NR, Yashar CM, Arend R, et al. NCCN Guidelines® Insights: Cervical Cancer, Version 1.2024: Featured Updates to the NCCN Guidelines[J]. J Natl Compr Canc Netw. 2023;21(12):1224–33.
4. Gadducci A, Cosio S. Neoadjuvant Chemotherapy in Locally Advanced Cervical Cancer: Review of the Literature and Perspectives of Clinical Research[J]. Anticancer Res. 2020;40(9):4819–28.
5. Pötter R, Tanderup K, Schmid MP, et al. MRI-guided adaptive brachytherapy in locally advanced cervical cancer (EMBRACE-I): a multicentre prospective cohort study[J]. Lancet Oncol. 2021;22(4):538–47.
6. Lakhman Y, Aherne EA, Jayaprakasam VS, et al. Staging of Cervical Cancer: A Practical Approach Using MRI and FDG PET[J]. Am J Roentgenol. 2023;221(5):633–48.
7. Haldorsen IS, Lura N, Blaakær J, et al. What Is the Role of Imaging at Primary Diagnostic Work-Up in Uterine Cervical Cancer?[J]. Curr Oncol Rep. 2019;21(9):77.
8. Fournier LS, Bats AS, Durdux C, Diffusion MRI. Technical principles and application to uterine cervical cancer[J]. Cancer/Radiothérapie. 2020;24(5):368–73.
9. Zhou J, Heo H, Knutsson L, et al. APT-weighted MRI: Techniques, current neuro applications, and challenging issues[J]. J Magn Reson Imaging. 2019;50(2):347–64.
10. Zhou J, Zaiss M, Knutsson L, et al. Review and consensus recommendations on clinical APT - weighted imaging approaches at 3T: Application to brain tumors[J]. Magn Reson Med. 2022;88(2):546–74.
11. Gao S, Du S, Lu Z, et al. Multiparametric PET/MR (PET and MR-IVIM) for the evaluation of early treatment response and prediction of tumor recurrence in patients with locally advanced cervical cancer[J]. Eur Radiol. 2020;30(2):1191–201.
12. Dolciami M, Capuani S, Celli V, et al. Intravoxel Incoherent Motion (IVIM) MR Quantification in Locally Advanced Cervical Cancer (LACC): Preliminary Study on Assessment of Tumor Aggressiveness and Response to Neoadjuvant Chemotherapy[J]. J Personalized Med. 2022;12(4):638.
13. Dappa E, Elger T, Hasenburg A, et al. The value of advanced MRI techniques in the assessment of cervical cancer: a review[J]. Insights into Imaging. 2017;8(5):471–81.
14. Reynolds HM, Tadimalla S, Wang YF, et al. Semi-quantitative and quantitative dynamic contrast-enhanced (DCE) MRI parameters as prostate cancer imaging biomarkers for biologically targeted radiation therapy[J]. Cancer Imaging: Official Publication Int Cancer Imaging Soc. 2022;22(1):71.
15. Perucho JA, U, Wang M, Vardhanabhuti V, et al. Association between IVIM parameters and treatment response in locally advanced squamous cell cervical cancer treated by chemoradiotherapy[J]. Eur Radiol. 2021;31(10):7845–54.
16. Zhang Y, Zhang K, Jia H, et al. IVIM-DWI and MRI-based radiomics in cervical cancer: Prediction of concurrent chemoradiotherapy sensitivity in combination with clinical prognostic factors[J]. Magn Reson Imaging. 2022;91:37–44.

17. Zhou J, Zaiss M, Knutsson L, et al. Review and consensus recommendations on clinical APT-weighted imaging approaches at 3T: Application to brain tumors[J]. Magn Reson Med. 2022;88(2):546–74.
18. Li S, Liu J, Zhang Z, et al. Added-value of 3D amide proton transfer MRI in assessing prognostic factors of cervical cancer: a comparative study with multiple model diffusion-weighted imaging[J]. Quant Imaging Med Surg. 2023;13(12):8157–72.
19. Song Q, Tian S, Ma C, et al. Amide proton transfer weighted imaging combined with dynamic contrast-enhanced MRI in predicting lymphovascular space invasion and deep stromal invasion of IB1-IIA1 cervical cancer[J]. Front Oncol. 2022;12:916846.
20. Zhou J, Heo HY, Knutsson L, et al. APT-weighted MRI: Techniques, current neuro applications, and challenging issues[J]. J Magn Reson imaging: JMRI. 2019;50(2):347–64.
21. Nichelli L, Zaiss M, Casagranda S. APT weighted imaging in diffuse gliomas[J]. BJR open. 2023;5(1):20230025.
22. Li B, Sun H, Zhang S, et al. The utility of APT and IVIM in the diagnosis and differentiation of squamous cell carcinoma of the cervix: A pilot study[J]. Magn Reson Imaging. 2019;63:105–13.
23. Yang C, Hassan HA, Omar NF, et al. The value of multi-parameters MRI based on amide proton transfer imaging in evaluating the efficacy of concurrent radiochemotherapy for locally advanced cervical cancer[J]. Magn Reson Imaging. 2025;123:110507.
24. Vickers AJ, Van Calster B, Steyerberg EW. Net benefit approaches to the evaluation of prediction models, molecular markers, and diagnostic tests[J]. Volume 352. BMJ (Clinical research ed.); 2016. p. i6.

# Figures

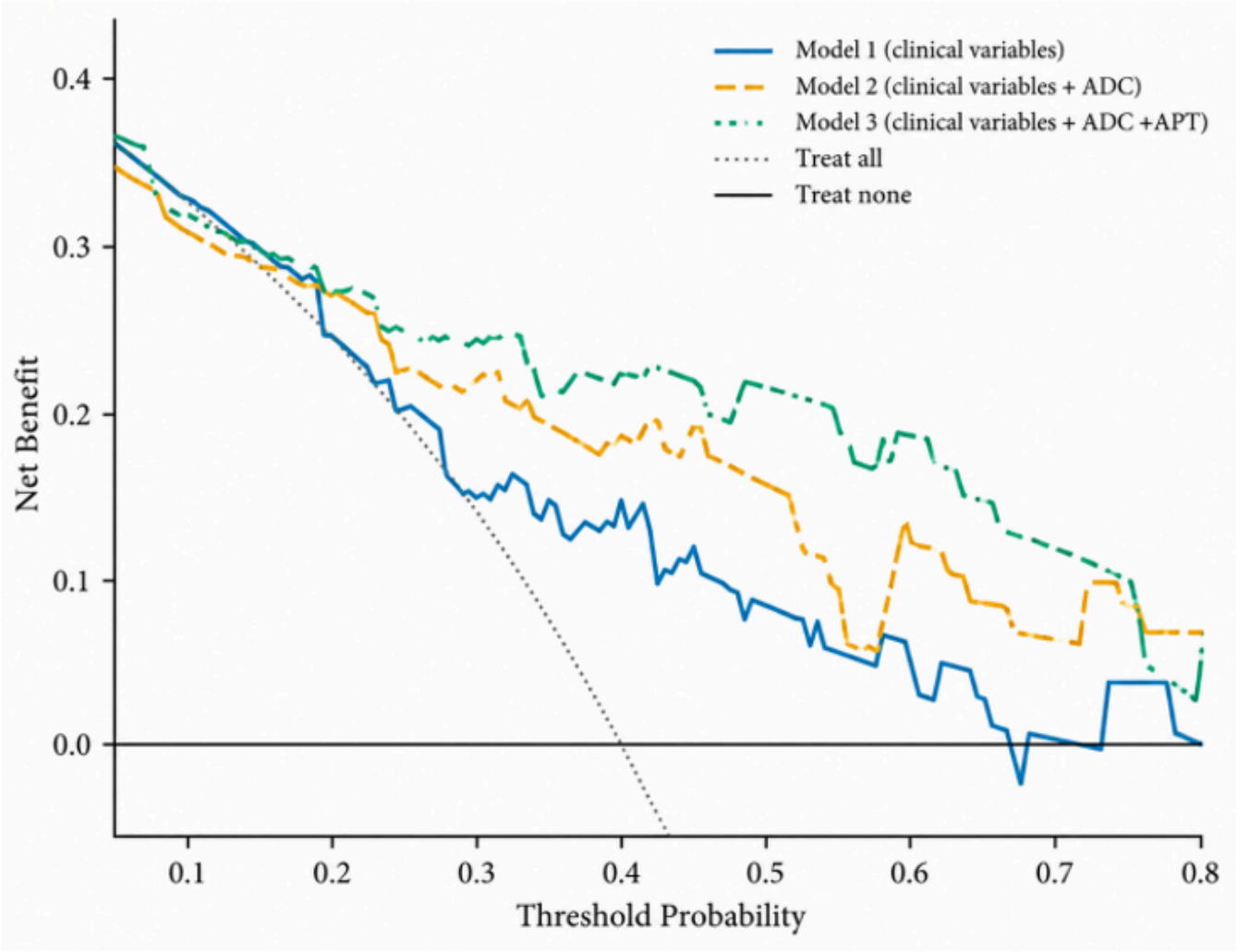


**Figure 4**

Decision curve analysis of the three predictive models for CCRT response in patients with cervical SCC.